Energy Losses in Photovoltaic-Thermoelectric Hybrid System with and without Solar Concentrator

M. MEJDAL[1], A. EL HARFOUF[1], M. NFAOUI [1], S. HAYANI-MOUNIR [1], K. CHOUKAIRY [2], K. EL-HAMI [3]

[1]Multidisciplinary Laboratory of Research And Innovation (LaMRI), EMAFI Team,
University of Sultan Moulay Slimane,
Polydisciplinary Faculty in Khouribga,
MOROCCO

[2]Process Engineering, Computer Science and Mathematics Laboratory (LIPIM),
University of Sultan Moulay Slimane, ENSA in Khouribga,
MOROCCO

[3]Scientific Institute,
Mohammed V University,
Rabat,
MOROCCO

Abstract: - A large part of solar irradiation is lost in different forms in the photovoltaic system hybridized with a TEG thermoelectric generator. This is disadvantageous for the best contribution of the TEG generator. The losses occur mainly on the front and rear of the PV-TEG hybrid system. They are usually radiation losses, natural convection losses, and forced convection losses due to the wind. In this paper, we studied the interaction of these different losses in both faces of the hybrid system according to different environmental factors such as solar radiation, ambient temperature, and wind speed. This study concerns two types of PV-TEG hybrid systems, the PV-TEG system with an optical concentrator and the one without an optical concentrator. It aims to determine the influence of environmental factors on these different losses and also to determine the dominant losses in both types of the PV-TEG hybrid system. The determination of the dominant losses and the estimation of their quantity makes it possible to make decisions for the optimization of these two hybrid systems, by adding solutions to reduce these dominant losses and transferring it towards the thermoelectric generator so that it can generate more electric power, and by avoiding that, these solutions strongly influence the performance of these two hybrid systems. For this purpose, an appropriate model is developed which includes all these losses.

Key-Words: - Photovoltaic, Thermoelectric, solar energy, thermal energy, Hybrid system, energy recovery, wasted energy, thermal losses.

Received: June 8, 2024. Revised: November 18, 2024. Accepted: December 9, 2024. Published: April 30, 2025.

1 Introduction

Science has proven the possibility of using solar energy by converting it into useful energy that humanity can benefit from. Attention has shifted to using solar energy; as it is characterized by its cleanliness and environmental friendliness, since it does not adversely affect the environment. Designed photovoltaic cells (PV cells) are renowned for their ability to convert incident solar radiation directly into electric power. In spite of this, an enormous portion of incident radiation is turned into dissipated heat instead of being converted into electric power by PV cells, [1].

To increase solar radiation conversion into useful power, PV cells are usually mixed with other systems, [2]. Among the ideas that have been applied to PV cells is to harness the induced heat by making it useful. For example, research papers have been conducted on the applicability of thermoelectric devices (TEG) to render the amount of heat produced by PV cells useful by turning it into additional power, [3]. When a TEG device is affixed behind the PV cell, its upper side temperature differs from that of its lower side due to the produced heat, this produces an electrical potential difference, [4].

In literature, research papers have been aimed study at studying the efficacy of combining a PV system with a TEG device [5], [6], [7]. The researchers in [5] have made a TEG devise behind the PV cell and determined its efficiency in converting solar radiation into electrical power. The results of this study [5] showed that the ability of the PV-TEG composed system to convert solar energy has improved by 23% compared to a single PV panel. Other work [6] also reached positive results, by confirming a 10% improvement in the efficiency of the PV-TEG composed system in converting solar energy into electrical energy. The dye-sensitized (DSSC) cell was used in the PV-TEG composed system for this work [6] as a PV cell.

Also, to raise the efficacy of this PV-TEG composed system in producing electrical energy, efforts have been made to make improvements to it. Whereas, the researchers in [7] added an inserted selective absorber between the DSSC cell and the TEG device, which led to a 13% improvement in efficiency.

To augment the electrical power of the PV-TEG composed system with Si cells, the researchers in the paper [8] added water pipelines to cool the TEG underside. They found that the electrical power produced by the new PV-TEG composed system increased by 30% if we compare it with that of the Si cells working alone under the same conditions. A different design was made by the researchers in [9], in which they placed a heat-pipe-based under a set of PV cells to cool it down and also to supply the TEG underside with the heat drawn. The new design showed an additional improvement compared to the same PV cells working alone.

The authors of [10] studied the effect of parameters on the PV-TEG composed system, i.e., PV cell current, radiation, and TEG structural parameters. The work elaborated in [10] also concluded that the performance of the PV-TEG composed system is advantageous compared to the PV cell working alone. The results confirm that the PV-TEG composed system with si-cell as a PV cell is advantageous compared to the same PV cell working without an additional system.

Another idea that has been tested theoretically and experimentally on the PV-TEG composed system is based on the use of a spectrum splitter, [11], [12], [13], [14], [15], [16], [17]. The technology is mainly based on dividing the incoming solar radiation into short wavelengths that are transmitted to the PV cell while the long wavelengths are reflected on the TEG device. This technique has shown its potential to improve the efficacy of the PV-TEG composed system, [12].

To increase the electric power of the PV-TEG composed system, a concentrator for the incoming solar radiation has been adopted by several researches, [18], [19], [20], [21]. The results revealed that the PV-TEG composed system with a solar concentrator could provide more electrical power compared to a CPV cell without a TEG device, [18].

Authors in [22], [23] built a novel PV-PCM-TEG composed system with phase-changing material PCM. The results proved that adding PCM to the PV-TEG composed system improved its performance.

All the mentioned studies mainly focus on the electrical power produced and on the efficiency along with optimization of the PV-TEG hybrid system composed of PV and TEG devices. Nevertheless, the analysis of energy losses that occur in PV-TEG composed systems has not attracted interest. Besides, identifying all types of losses, their percentage and quantity, which are as follows: radiation loss, forced convection loss, and natural convection loss. These energy losses that take place on the upper and lower sides of the PV-TEG composed system were incorporated into the mathematical model of our study.

Our previous paper [24], it was shown that meteorological variables can affect the ability of the PV-TEG composed system to generate power, which are wind, ambient temperature, and solar radiation. Thus, the wasted energy must be studied by changing these climatic factors. This will allow us to observe the change of each type of loss occurring and to identify the dominant loss and the conditions and causes of its dominance.

Our study gives a deep vision the wasted energy in the PV-TEG composed system, by defining the percentage and magnitude of each energy loss. The forms of wasted energy that have been studied are as follows: energy lost by radiation, energy wasted by forced convection, and energy lost by natural convection. All these wasted energy forms eventuating in the upper and lower sides of PV-TEG composed system are evaluated by changing wind speed, ambient temperature, and solar radiation.

2 System Description

The hybrid system we are about to study is a direct combination of two systems that can generate electrical energy through different processes. These two systems are, on the one hand, the PV cell directly affixed to the upper interface of the TEG system, as shown in Figure 1.

As for the PV cell, it consists of 5 layers. So that the first layer exposed to solar radiation is a transparent glass followed by an EVA layer which is also transparent, directly below it we find crystalline silicon cells responsible for converting part of the incoming solar radiation into useful electrical energy and another part into thermal energy, under it we find another layer of EVA and directly we find the final layer, which is the tedlar.

As for the TEG system, it consists of an upper layer of ceramic that is attached to the tedlar layer of the PV cell, followed by a group of small confluent units made up of p-type and n-type semiconductors material, which are electrically assembled in series, which is responsible for converting thermal energy into additional electrical energy. Immediately after these units, we find another lower ceramic layer.

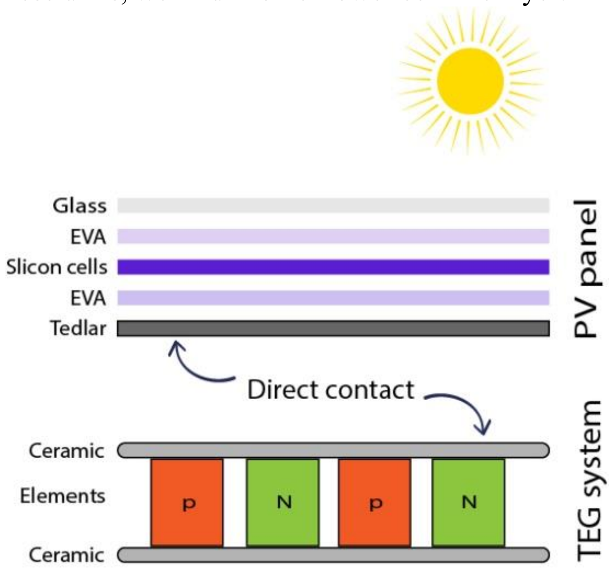

Fig. 1: Layers constituting the PV-TEG hybrid system

3 Types of Wasted Energy

The study deals with determining the change of the lost energy in terms of the meteorological variables for the PV-TEG hybrid system. Hence, it is necessary to identify the different forms in which thermal energy is lost on the one hand, and on the other hand, the places in which the energy is lost. For our study, we consider that the loss occurs at the front and back facade due to the fact that its area is very large compared to the thickness of the system. As for the energy loss in this system, it is wasted in the form of radiation, natural convection and forced convection.

In this paragraph we will also present mathematical relations for each type of energy loss, as well as simulate it.

Table 1 presents information on the properties of the PV system used in this study.

Table 1. Values of the PV Panel Properties

Properties of the PV Panel	Symbol	Value
Area of PV Panel (m^2)	A_P	1
Thickness of glass (mm)	L_G	3 [25]
Thickness of EVA (mm)	L_E	0.5 [25]
Thickness of Silicon cell (mm)	L_S	0.4 [25]
Thickness of tedlar (mm)	L_t	0.1 [25]
Thermal conductivity of glass (W/m.K)	k_g	0.9 [25]
Thermal conductivity of EVA (W/m.K)	k_E	0.35 [25]
Thermal conductivity of Silicon cell (W/m.K)	k_S	148 [25]
Thermal conductivity tedlar (W/m.K)	k_t	0.2 [25]
The emissivity of silicon cell	ϵ_s	0.9 [25]
Efficiency at a reference condition	η_{ref}	18.4 % [26]
Solar cell temperature coefficient	β	0.0038 [26]
Absorptivity of glass	ϵ_g	0.02[27]

3.1 Energy Wasted in PV Panel

When we put the PV cells in sunlight, they start to generate electrical energy with the photovoltaic effect. But the bulk of the solar energy will be converted into heat. Some of this heat is transferred by conduction to the TEG system, while the rest is lost to the upper facade of the PV cells. This heat loss takes place in the form of natural convection, and forced convection due to the presence of wind and radiation loss, as shown in Figure 2. Regarding radiation loss, it is divided into two parts, radiation loss in the direction of the sky and radiation loss in the direction of the ground, because the hybrid system is often tilted at a certain angle.

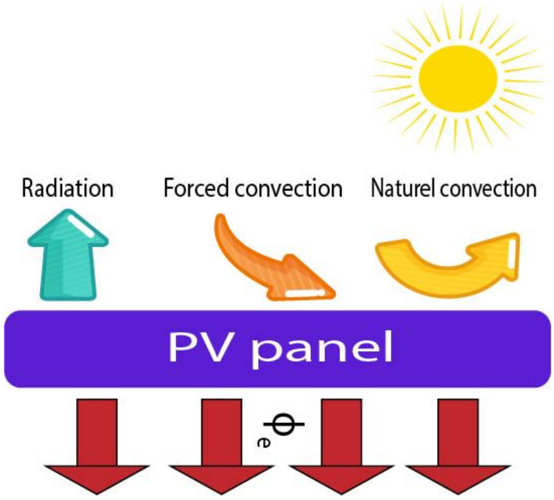

Fig. 2: Heat transfer mechanisms occurring at the Frontend of the PV system

3.1.1 Energy Wasted by Forced Convection

For the energy loss in the form of forced convection due to the wind, it is calculated by the following relation:

$$Q_{F,g} = h_w A_P \left(T_g - T_a\right) \quad 1)$$

- A_P: is the area of the PV cells.
- T_g: temperature of the upper surface of the solar cells.
- T_a: ambient temperature.
- h_w: coefficient of heat transfer for forced convection which is due to wind speed [28]:

$$h_w = 5.678\left\{a + b\left[\frac{\left(\frac{294.26}{273.16 + T_a}\right)V}{0.3048}\right]^n\right\} \quad (2)$$

- a, b, and n are constant values given by reference, [29].
- V: wind velocity.

According to Relation No (1) and (2), the energy lost due to the wind is related to the temperature of the glass and that of the ambient and the wind speed. To find out the response of this type of lost energy, we simulated it according to the change in wind speed and ambient temperature with respect to a fixed glass temperature.

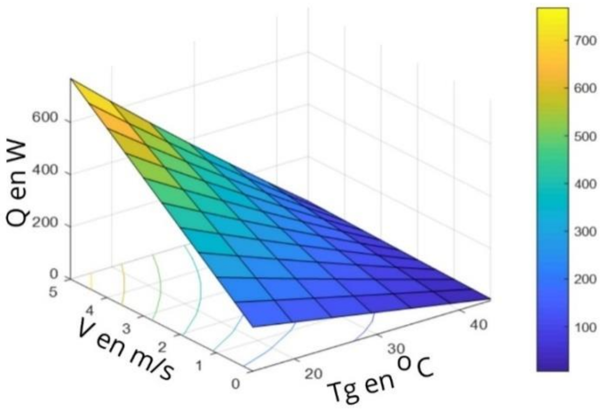

Fig. 3: Simulations of lost energy by forced convection due to wind as a function of ambient temperature and wind velocity with a glass temperature Ta=20

Figure 3 gives a representative result of this simulation. The energy lost, according to Figure 3, appears to be more important as wind speeds increase and ambient temperature decreases. This is due to the fact that the loss coefficient is related to the wind speed according to relation N 2, as well as the fact that the decrease in the ambient temperature, considering the glass temperature fixed, makes the difference between them increase according to relation N 1. So, the decrease in the ambient temperature and the high wind speed are the factors that motivate the increase of energy loss.

3.1.2 Energy Wasted by Natural Convection

The lost energy by natural convection can be calculated by the following relation:

$$Q_{N,g} = A_P h_{N,g} \left(T_g - T_a\right) \quad (3)$$

$h_{N,g}$: The heat transfer coefficient for natural convection in the upper surface of the hybrid system is [30]:

$$h_{N,g} = 0.14\frac{k_a}{L}\left[\left(GrPr\right)^{1/3} + \left(Gr_{cr}Pr\right)^{1/3} + 0.56\left(Gr_{cr}Pr\cos\theta\right)^{1/4}\right] \quad (4)$$

With:

- Gr_{cr}: the Critical number.
- Gr: Grashof number.
- Pr: Prandtl number.

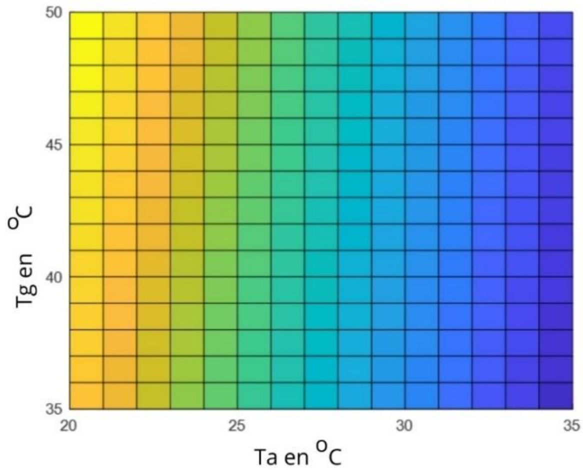

Fig. 4: Simulations of lost energy by natural convection as a function of ambient temperature and glass temperature

As shown in relation No (3), the lost energy by natural convection is related to ambient and glass temperature. To get an idea of how this wasted energy is affected by these factors we simulate it in Figure 4. According to Figure 4, it appears that the energy wasted by natural convection is very important at a low ambient temperature and more important when the glass temperature is also high. Thus, the decrease in the ambient temperature along with the rise in the glass temperature are factors that increase the importance of the energy lost by natural convection.

3.1.3 Energy Wasted by Radiation

As for the losses of radiation towards the sky and towards the ground, they are respectively as follows:

$$Q_{R,P,gro} = \frac{\left(T_P - T_{gro}\right)}{R_{R,P,gro}} \quad (5)$$

$$Q_{R,P,sky} = \frac{\left(T_P - T_{sky}\right)}{R_{R,P,sky}} \quad (6)$$

with:

- T_P: Temperature of the upper surface of the solar cells.
- T_{gro}: represents the temperature of the ground which is often taken with a value equal to ambient temperature $T_{gro}=T_a$ [31], [32].
- T_{sky}: refers to the temperature of the sky, [33]:

$$T_{sky} = 0.0552\ T_a^{3/2} \quad (7)$$

- $R_{R,P,gro}$: radiation resistance on the top of the crystalline cell toward the ground.

$$R_{R,P,gro} = \frac{1}{\epsilon_g F_{P,gro} \sigma A_{PV}(T_P+T_{gro})(T_P^2+T_{gro}^2)} \quad (8)$$

- $R_{R,P,sky}$: radiation resistance on the top of the crystalline cell toward the sky.

$$R_{R,P,sky} = \frac{1}{\epsilon_g F_{P,sky} \sigma A_{PV}(T_P+T_{sky})(T_P^2+T_{sky}^2)} \quad (9)$$

- ϵ_g is the glass emissivity.
- σ is the Stefan-Boltzmann constant.
- $F_{P,gro}$ and $F_{P,sky}$ are respectively configuration factors of the ground and the sky:

$$F_{P,gro} = \frac{1}{2}\left(1-\cos(\theta)\right) \quad (10)$$

$$F_{P,sky} = \frac{1}{2}\left(1+\cos(\theta)\right) \quad (11)$$

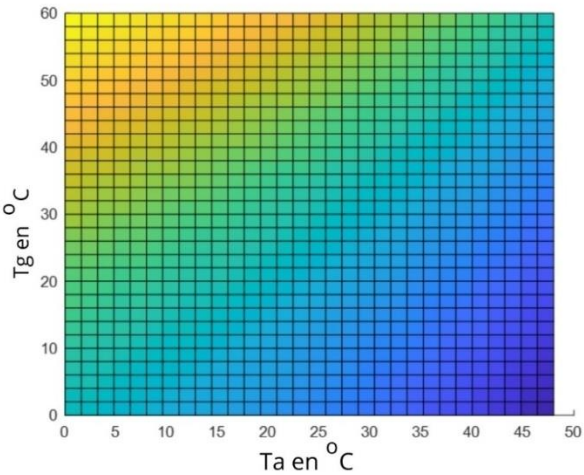

Fig. 5: Simulations of lost energy by radiation as a function of ambient temperature and glass temperature

Figure 5 represents a simulation of the wasted energy by radiation response in terms of ambient and PV cell temperature. The wasted energy represented here is the sum of the energy wasted by radiation towards the sky and that towards the ground. It is clear in Figure 5 that the radiation wasted energy is very important at a PV cell's high temperature and at a very low ambient temperature.

The simulations that we have done show the factors that affect the various types of energy losses that we study in this paper. They are, however, insufficient to demonstrate the individual response to these energy losses during the operation of the combined PV-TEG system. Therefore, to study these energy losses, it is necessary to provide a mathematical representation of the PV-TEG integrated system that enables us to simulate these types of energy losses, which is the subject of the next paragraphs.

3.2 Energy Wasted in the TEG System

After the TEG system receives the heat induced by the PV panel, the latter produces additional electrical energy. However, a significant portion of this heat will be lost on the back facade after it has passed through its component layers. When it reaches the back facade of the TEG system, it is lost by forced convection induced by the wind, by natural convection and then by radiation as shown in Figure 6. As for the radiation loss, it will also be divided into radiation loss towards the sky and then towards the ground.

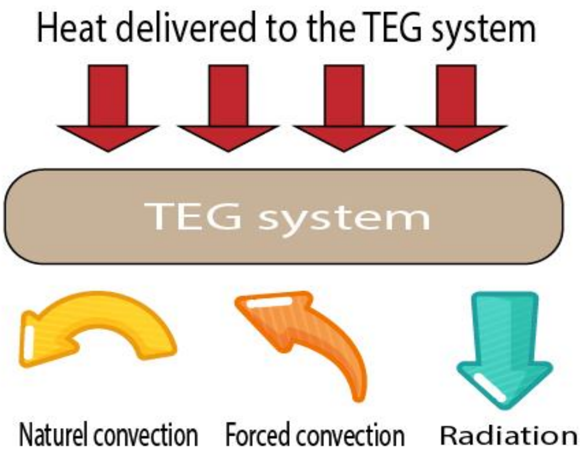

Fig. 6: Heat transfer mechanisms occurring at the backend of the TEG system

Table 2 presents information on the properties of the TEG system used in this study.

Table 2. Values of the TEG system Properties

Properties of the TEG system	Symbol	Value
Area of 30 thermocouple	A_{TE}	$0.01m^2$ [34]
Thickness of ceramic	L_c	0.2 mm [25]
Thickness of thermoelectric units	L_{TE}	1 mm [25]
Thermal conductivity of Ceramic	k_c	30 (W/m.K) [25]
Thermal conductivity of thermoelectric units	k_{TE}	$2\times(930.6T - 1.981T^2) \times 10^{-9}$ W/m.K [27]
Seebeck coefficient	S	$(44448.0+1861.2Ta-981T^2) \times 10^{-9}$ V K^{-1} [27]
Electrical resistivity	ρ	$2\times(5112+163.4T - 0.6279Ta^2)\times10^{-10}$ Ω·m [27]
Thomson coefficient	μ	$2 \times (930.6T - 1.981T^2) \times 10^{-9}$ (V/K) [27]
The emissivity of the ceramic	ϵ_c	0.85 [25]

3.2.1 Energy Wasted by Forced Convection

For the energy loss in the form of forced convection due to the wind, it is calculated by the following relation:

$$Q_{F,cr} = h_w A_{TE} \left(T_{cr} - T_a\right) \tag{12}$$

- T_{cr}: represents the temperature of the down surface of the ceramic layer.
- A_{TE}: area of the back façade of the TEG system.

3.2.2 Energy Wasted by Natural Convection

The lost energy by natural convection can be calculated by the following relation:

$$Q_{N,cr} = A_{PV} h_{N,cr} \left(T_{cr} - T_a\right) \tag{13}$$

$h_{N,cr}$ refers to the natural heat transfer coefficient [30]:

$$h_{N,cr} = \left[0.825 + \frac{0.387 Ra^{1/6}}{\left[1+\left(0.492/Pr\right)^{8/16}\right]^{8/27}}\right]^2 \frac{k_a}{L} \tag{14}$$

- Ra is Rayleigh number.

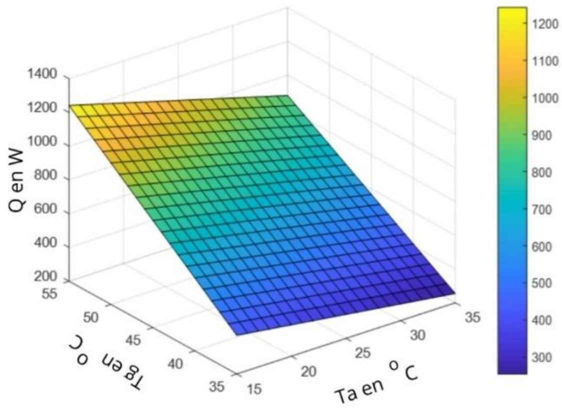

Fig. 7: Simulations of lost energy by natural convection as a function of ambient temperature and glass temperature

As per Figure 7, the wasted energy by natural convection at the back side is important at low ambient temperature and high ceramic temperature.

3.2.3 Energy Wasted by Radiation

As for the losses of radiation towards the sky and towards the ground, they are respectively as follows:

$$Q_{R,cr,gro} = \frac{\left(T_{cr} - T_{gro}\right)}{R_{R,cr,gro}} \tag{15}$$

$$Q_{R,cr,sky} = \frac{\left(T_{cr} - T_{sky}\right)}{R_{R,cr,sky}} \tag{16}$$

- $R_{R,cr,gro}$: the radiation resistance on the bottom of ceramic layer toward the ground.

$$R_{r,cr,gro} = \frac{1}{\epsilon_{cr} F_{cr,gro} \sigma A_{PV} (T_{cr}+T_{gro})(T_{cr}^2+T_{gro}^2)} \tag{17}$$

- $R_{R,cr,sky}$: the radiation resistance on the bottom of the ceramic layer toward the sky.

$$R_{r,cr,sky} = \frac{1}{\epsilon_{cr} F_{cr,sky} \sigma A_{PV} (T_{cr}+T_{sky})(T_{cr}^2+T_{sky}^2)} \tag{18}$$

- $F_{cr,gro}$ and $F_{cr,sky}$ are, respectively, the configuration factors for the ground and the sky.

$$F_{cr,gro} = \frac{1}{2}\left(1-\cos\left(\pi-\theta\right)\right) \tag{19}$$

$$F_{cr,sky} = \frac{1}{2}\left(1+\cos\left(\pi-\theta\right)\right) \tag{20}$$

4 Energy Balance Equations

This part which is interested in the modeling of energy transfer is divided into 5 sections namely; Energy balance equation for (1) the upper facade of glass, (2) the upper facade of silicon cell (3) the upper facade of thermoelectric units (4) lower facade of thermoelectric units (4) down facade of ceramic layer.

The energy equations extracted are based on the application of the energy balance on 5 surfaces of the hybrid system. The choice of the 5 surfaces is mainly based on the calculation of the temperature necessary to calculate each type of energy lost, which are:

- T_g: temperature of the upper surface of the glass.
- T_P: Temperature of the upper surface of silicon cells.
- T_H: Temperature of the hot side of thermoelectric units.
- T_C: Temperature of the cold side of thermoelectric units.
- T_{cr}: Temperature of the down surface of the ceramic layer.

As for the thermal resistance of each group of layers R_j, it is written as follows:

$$R_j = \sum_i^n \frac{L_i}{A_i k_i} \quad (21)$$

Such as:

- i: Name of each layer.
- j: Name of each group of layers.
- L_i: Length of layer type i.
- k_i: Conductivity of layer type i.

4.1 Energy Balance Equation for the Upper Facade of Glass

When the solar radiation G passes through the layers of the photovoltaic panel, a part of it is absorbed by the glass $G_\alpha = G\ \alpha_g$ where α_g is the glass absorption coefficient. The generated heat by conduction through EVA and glass layers is denoted as $Q_{EVA\text{-}g}$ and it is lost on the surface of the glass by natural convection $Q_{N,g}$, and forced convection $Q_{F,g}$.

The expression of $Q_{EVA\text{-}g}$ is as follows:

$$Q_{EVA-g} = \frac{\left(T_P - T_g\right)}{R_{EVA-g}} \quad (22)$$

- $R_{EVA\text{-}g}$: represents the thermal resistance of the EVA and the glass, which is expressed using equation (21).

The following equation describes the energy balance for the upper facade of glass:

$$0 = Ga\ A_P + \frac{\left(T_P - T_g\right)}{R_{EVA-g}} - h_w A_P \left(T_g - T_a\right) - A_P h_{N,g} \left(T_g - T_a\right) \quad (23)$$

4.2 Energy Balance Equation for the Upper Facade of Silicon Cell

When the transmitted radiation G_t reaches the solar cell, a part of it is converted into electricity P_{PV} through the photovoltaic effect, and the other part is absorbed $G(\alpha_P\ \tau_g)$ by the cell material where α_P is the solar cell absorption coefficient and τ_g is the transmissivity of the glass.

A portion of absorbed energy by cell material is lost in the ambient atmosphere by radiation to the ground $Q_{R,P,gro}$, radiation to the sky $Q_{R,PV,sky}$, and by conduction $Q_{EVA\text{-}g}$ through EVA and glass. The remaining part of the energy, which is noted as $Q_{P\text{-}EVA\text{-}t\text{-}cr}$, passes through the solar cell towards the EVA, the tedlar, and the top ceramic layers

The expression of each heat flow is as follows:

$$Q_{P,EVA,t,cr} = \frac{\left(T_P - T_H\right)}{R_{P,EVA,t,cr}} \quad (24)$$

- $R_{P,EVA,td,cr}$ Represents the thermal resistance of the silicon cell, EVA, tedlar and ceramic layers, which is expressed using equation (21).

$$P_P = A_P\ G\ \eta_P \quad (25)$$

- η_p: Efficiency of PV cell [27]:

$$\eta_p = \eta_{ref}\left[1 - \beta_{ref}\left(T_P - T_{ref}\right)\right] \quad (26)$$

- η_{ref}: PV cell efficiency at the reference temperature T_{ref}=25°C, and reference solar radiation G_{ref}=1000W/m^2.
- β_{ref}: Coefficient of temperature dependency of the cell.

The following equation describes the energy balance for the upper facade of the silicon cell:

$$0 = -\frac{\left(T_P - T_{cr}\right)}{R_{P,EVA,t,cr}} + G\left(\alpha_{PV}\tau_g\right)A_{PV} - \frac{\left(T_P - T_g\right)}{R_{EVA-g}} - \frac{\left(T_P - T_{gro}\right)}{R_{R,P,gro}} - \frac{\left(T_P - T_{sky}\right)}{R_{R,P,sky}} - P_P \quad (27)$$

4.3 Energy Balance Equation for the Upper Facade of Thermoelectric Units

Firstly, the thermal contact between the thermoelectric module and the PV module is supposed to be perfect, so that the heat, which passes down the PV module $Q_{P\text{-}EVA\text{-}t\text{-}cr}$, will be completely delivered to the TEG generator Q_h. The heat through the hot side of the thermoelectric units Q_h can be written as follows, [27]:

$$Q_H = n_{TE}\left(\begin{array}{l} s\left(T_H\right)I_{TE}T_H - \dfrac{I_{TE}^2 R_{TE}}{2} + \dfrac{\left(T_H - T_c\right)}{R_{TE}} \\ -\dfrac{\mu\left(T_c\right)I_{TE}\left(T_H - T_c\right)}{2} \end{array}\right) \quad (28)$$

- I_{TE}: Electrical current passing through the

TEG element [27].

$$I_{TE} = \frac{n_{TE}\left[\left(s(T_H)T_H - s(T_c)T_c\right) - \mu\left(T_H - T_c\right)\right]}{n_{TE}\ R_{TE} + R_C} \quad (29)$$

- R_{TE}: Resistance of the thermoelectric units.
- R_C: Load resistance is taken equal to R_{TE}.
- n_{TE}: is the number of thermoelectric elements. It is determined by obtaining a surface equal to that of the PV cell 1 m^2.
- The properties of temperature dependency for the bismuth telluride (Seebeck coefficient s(T), Thomson coefficient $\mu(T)$ and resistivity coefficient $\rho(T)$ are given by [27].

The heat, which passes down the PV module $Q_{PV\text{-}EVA\text{-}t\text{-}cr}$, will be completely delivered to the TEG generator Q_h:

$$Q_{P,EVA,t,cr} = Q_H \quad (30)$$

$$\frac{(T_P - T_H)}{R_{P,EVA,t,cr}} = n_{TE}\begin{pmatrix} s(T_H)I_{TE}T_H - \frac{I_{TE}^2 R_{TE}}{2} + \frac{(T_H - T_c)}{R_{TE}} \\ -\frac{\mu(T_c)I_{TE}(T_H - T_c)}{2} \end{pmatrix} \quad (31)$$

4.4 Energy Balance Equation for the Lower Facade of Thermoelectric Units

By taking advantage of thermal energy Q_h, the thermoelectric units will produce an electrical power P_{TE}, whereas the heat flow leaving these thermoelectric units is Q_c. The heat through the cold side of the thermoelectric units Q_c can be written as follows, [27]:

$$Q_c = n_{TE}\begin{pmatrix} s(T_c)I_{TE}T_c + \frac{I_{TE}^2 R_{TE}}{2} + \frac{(T_H - T_c)}{R_{TE}} \\ +\frac{\mu(T_H)I_{TE}(T_H - T_c)}{2} \end{pmatrix} \quad (32)$$

The heat flow leaving the thermoelectric elements Q_c is equal to the heat that passes through the cold layer of ceramic Q_{cr}:

$$Q_c = Q_{cr} \quad (33)$$

$$Q_{cr} = \frac{(T_C - T_{cr})}{R_{cr}} \quad (34)$$

- R_{cr}: is the thermal resistance of the cold layer of ceramic, which is expressed using equation (21).

$$\frac{(T_C - T_{cr})}{R_{cr}} = n_{TE}\begin{pmatrix} s(T_c)I_{TE}T_c + \frac{I_{TE}^2 R_{TE}}{2} + \frac{(T_H - T_c)}{R_{TE}} \\ +\frac{\mu(T_H)I_{TE}(T_H - T_c)}{2} \end{pmatrix} \quad (35)$$

4.5 Energy Balance Equation for Ceramic Down Layer

Finally, the heat that passes through the cold layer of ceramic Q_{cr} will be dissipated by forced convection $Q_{F,cr}$, natural convection $Q_{N,cer}$ and radiation $Q_{R,cr}$ toward the sky $Q_{R,cr,sky}$ and toward the ground $Q_{R,cr,gro}$.

The following equation describes the energy balance for down façade of the cold ceramic layer:

$$0 = \frac{(T_C - T_{cr,b})}{R_{cr}} - \frac{(T_{cr} - T_{gro})}{R_{R,cr,gro}} - \frac{(T_{cr} - T_{sky})}{R_{R,cr,sky}} - h_w A_{TE}(T_{cr} - T_a) - A_p h_{N,cr}(T_{cr} - T_a) \quad (36)$$

Finally, the following equations that we have obtained: (23), (27), (32), (35) and (36) constitute a system of nonlinear equations. The resolution of this system with five nonlinear equations is obtained by applying the Newthon-Raphson method.

5 Results and Discussion

After identifying and describing the different types of energy loss that occur on both sides of the PV-TEG hybrid system, it can be seen from Figure 8, Figure 9 and Figure 10 that the energy lost by forced convection, by natural convection, or by radiation at the top and bottom surface of the PV-PV hybrid system depends on the values of the climatic factors.

To illustrate the behavior of each type of energy loss when a climatic factor changes, we simulated these losses as a function of ambient temperature, wind speed, and finally solar radiation separately.

To observe the variation of each type of lost energy, we fixed the value of wind velocity and solar radiation for four cases (G = 500 W / m^2; Vw = 4m/s, G = 1000 W / m^2; Vw = 1m/s, G = 500; Vw = 1m/s and G = 1000 W / m^2; Vw = 4m/s). We performed the simulation by switching the ambient temperature value between 0°C and 40°C. Figure 8, shows 4 simulations performed. In all simulations, the way of variation of all the types of lost energy considered in our study does not change. Whereas, the loss by convection at the front and rear of the PV-TEG hybrid system decreases linearly with the increasing value of the ambient temperature, while the loss by radiation on both sides increases its value linearly with the ambient temperature.

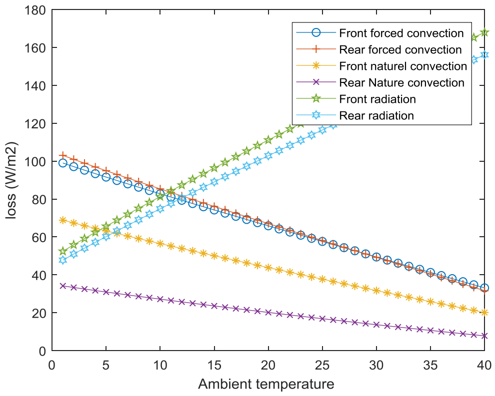

a

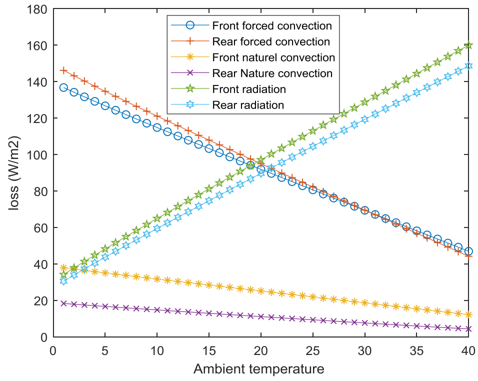

b

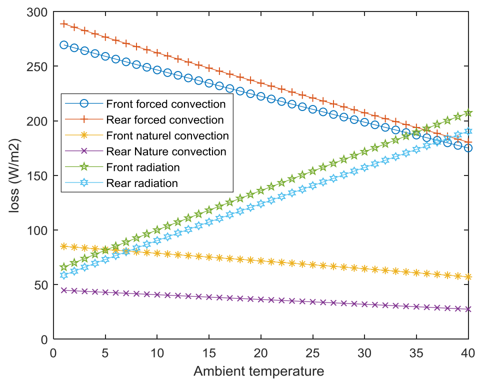

c

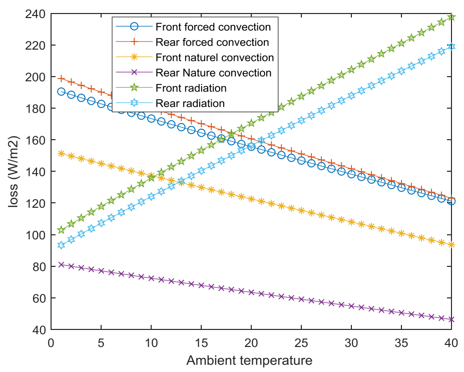

d

Fig. 8: Simulation of the energy losses in function of ambient temperature for a) G=500 W/m^2; Vw=1m/s b) G=500 W/m^2; Vw=4m/s c) G=1000 W/m^2; Vw=4m/s and d) G=1000 W/m^2; Vw=1m/s

It is noticeable that the loss by radiation and natural convection in the front facade is greater compared to the posterior facade. Overall, the total loss in the front facade is greater than the total loss in the back facade. It is noted in Figure 1 that when the wind speed is weak and the intensity of solar radiation is strong the radiation loss is dominant in both façades at a slight rise in the ambient temperature. This is explained by the fact that the PV-TEG hybrid system's temperature will be high due to the importance of the intensity of the incoming solar radiation, which becomes a large proportion of it to heat, and also because of the weak winds that cannot cool the system sufficiently. The elevated temperature of the PV-TEG hybrid system leads to the stimulation of radiation loss as the temperature of the PV-TEG hybrid system increases with the increase in the ambient temperature and the solar radiation intensity. These results confirm that, in all cases in regions of elevated temperature, radiation loss is predominant in the PV-TEG hybrid system.

Figure 9 shows two simulations made for the variation of the various energy losses when the intensity of solar radiation changes between 100 W/m^2 and 1000 W/m^2 for two cases (Vw=1m/s; Ta=10°C and Vw=1m/s; Ta=20°C). As per this figure, all studied energy losses change linearly and increase with increasing value of the solar radiation intensity. It is observed in this figure that the total losses at the front facade of the hybrid system are always greater compared to the posterior facade. Forced convection loss appears to tend to predominate with respect to low ambient temperature and high wind speed, while radiation loss predominates in the case of high ambient temperature and low wind speed.

It is noticeable that the loss by radiation and natural convection in the front facade is greater compared to the posterior facade, in contrast to what occurs with forced convection. Overall, the total loss in the front facade is greater than the total loss in the back facade. It is observed in all cases that forced convection tends to dominate in higher wind velocity values. Whereas, at a certain value of wind velocity, forced convection becomes dominant despite the high intensity of solar radiation (Figure 5 case b and d with G=1000w/m^2). This is explained by the fact that wind velocity is the catalyst for forced convection, as it increases with the increase in its values. This is evidenced by relation No. 45. Thus, regions with high wind velocities are predominantly with forced convection losses even at important radiation intensities such as 1000 W / m^2.

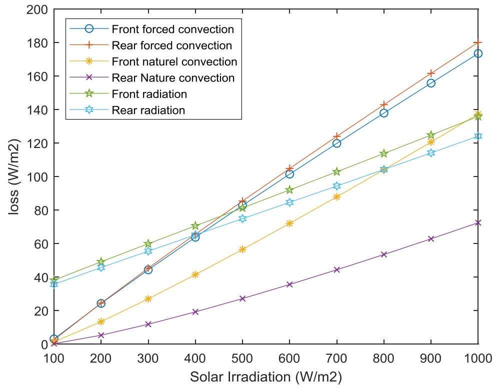

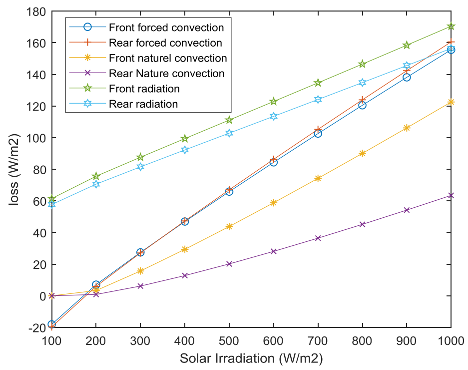

a

b

Fig. 9: Simulation of the energy losses in function of solar radiation for a) Vw=1m/s; Ta=10°C and b) Vw=1m/s; Ta=20˚C

As for Figure 11, it represents the change in energy loss with the change of the solar optical concentrator for 4 states Vw = 1 m/s; Ta = 10°C, Vw = 1 m/s; Ta = 20˚C, Vw = 4 m/s; Ta = 10˚C, Vw = 4 m/s; Ta = 20 °C. The change in energy loss by radiation appears to be exponential with the change in the optical concentration. Also, the energy lost by radiation at the front facade of the hybrid system is greater than that lost in the back facade. In addition, it clearly appears that radiation loss is dominant compared to the rest. In fact, the amount lost by radiation is much greater than the amount of energy lost for all types of energy losses combined, whether the ambient temperature and wind speed are high or low. Whereas for an optical concentration equal to C = 150, solar radiance equal to G = 600 W / m^2, wind velocity of Vw = 1 m / s and ambient temperature equal to Ta = 25 ˚C, the energy loss due to radiation in the front façade represents 40% and in the posterior façade represents 24% of the overall energy loss in the PV-TEG hybrid system with solar concentration as per Figure 12. For more details on the influence of the solar optical concentrator on the electrical productivity of the photovoltaic-thermoelectric hybrid system, refer to our article, [35].

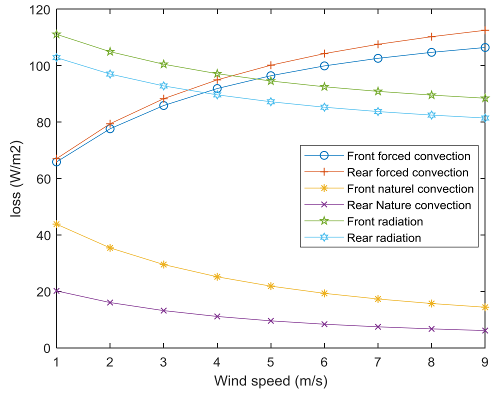

(a)

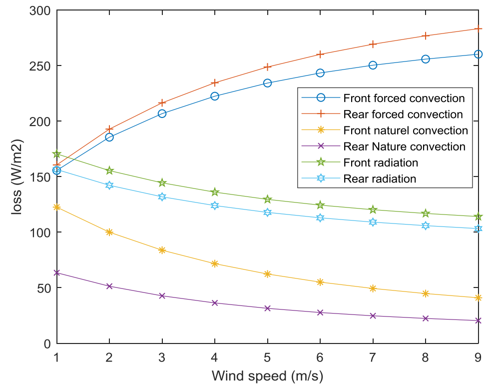

(b)

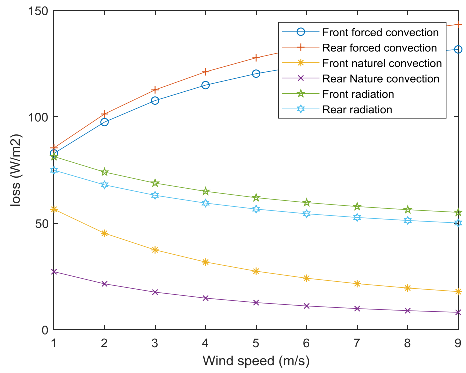

(c)

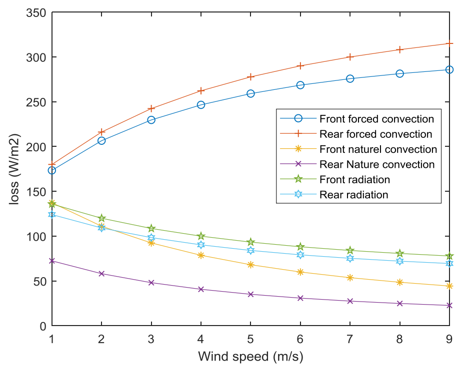

(d)

Fig. 10: Simulation of the energy losses in function of wind speed for a) G=500 W/m^2; Ta=20 ˚C b) G=1000 W/m^2; Ta=20 ˚C c) G=500 W/m^2; Ta=10 ˚C and d) G=1000 W/m^2; Ta=10 ˚C

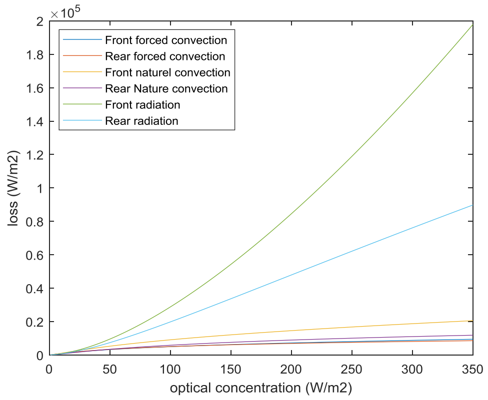

(a)

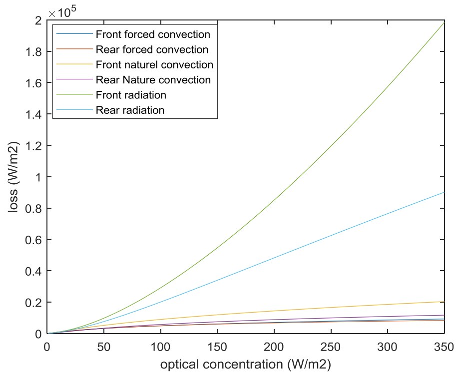

(b)

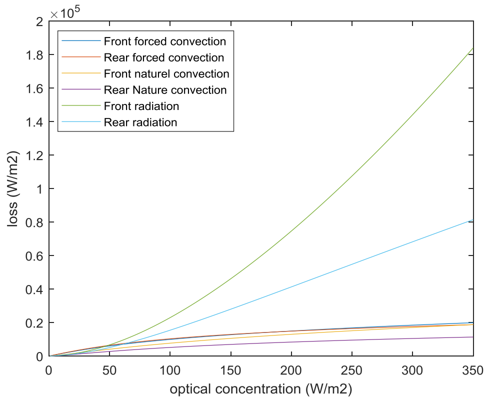

(c)

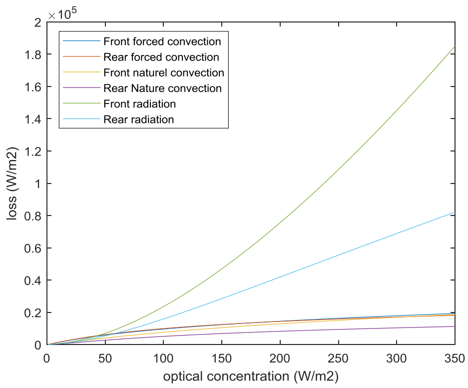

(d)

Fig. 11: Simulation of the energy losses in function of wind speed for a) G=500 W/m^2; Ta=20 ˚C, b) G=1000 W/m^2; Ta=20 ˚C c) G=500 W/m^2; Ta=10 ˚C and d) G=500 W/m^2; Ta=10 ˚C

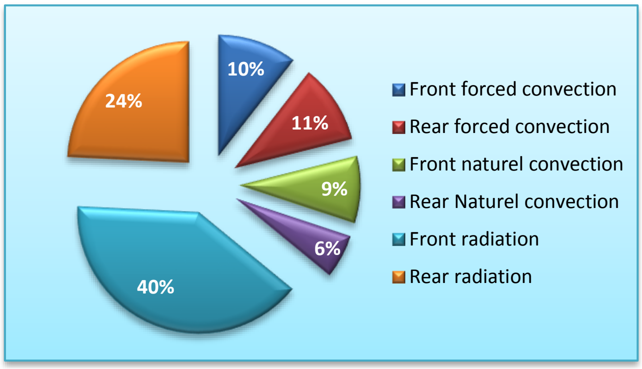

Fig. 12: Percentages of the different types of losses in relation to the total loss at the level of the PV-TEG hybrid system for C=150, G=600 W/m^2, Vw=1 m/s and Ta= 25 ˚C

From the results obtained, it is clear that the loss of thermal energy in the PV-TEG hybrid system is carried out through three processes that occur at the front and rear façade of the PV-TEG hybrid system. The thermal energy is lost either in the form of radiation or by natural convection or forced convection. These types of losses have a different appearance depending on the meteorological factors in which the PV-TEG hybrid system operates, as shown in Figure 8, Figure 9, Figure 10, Figure 11 and Figure 12. It was noted that the dominance conditions for each energy loss type differ.

In summary, Table 3 (Appendix) gives a classification of the conditions of dominance for each type of energy loss according to climatic factors.

6 Conclusion

This study is based on a mathematical model that takes into account various thermal losses such as natural and forced convection and radiation, and the various effects that occur during operation of the PV-TEG hybrid system. The study relates to two types of PV-TEG hybrid systems, the PV-TEG system with an optical concentrator and the one without an optical concentrator. From the obtained results, each form of wasted energy changes differently depending on the meteorological factors in which the PV-TEG hybrid system operates. The increase in the ambient temperature is enough to make the loss by radiation increase and be important while the loss of natural and forced convection decreases. Also, the high wind speed leads to an increase in the wasted energy by forced convection by virtue of the fact that the wind is responsible for this type of loss, while the loss decreases by radiation and natural convection. As for the value of the intensity of solar radiation, all types of energy loss increase with the increase of this climate parameter.

The obtained results also determine the areas and conditions of dominance for each type of energy loss. For example, hot regions, which are characterized by high temperature and high solar radiation, are dominated by radiation loss on both faces of the PV-TEG hybrid system. As for regions that are characterized by high wind speed and low temperature, and whether the solar radiation is high or low, we find that the loss by forced convection is dominant. When using an optical concentration, we find that in all cases the radiation loss is dominant and its value is very great.

This analysis of the wasted energy provides the possibility to determine the amount and percentage of the total energy loss as well as for each type of it and also enables the determination of the climatic conditions for the dominance of each type.

This analysis, along with its data, opens the door to finding innovative solutions based on it by making a suitable design for this PV-TEG hybrid system or adding ideas and devices to it in order to improve its efficiency in the conversion of solar energy into useful energy. This is in order to push the PV cells to work at their maximum capacity by lowering their temperature, as well as by transferring the greatest amount of heat to the TEG system at the same time.

Declaration of Generative AI and AI-assisted Technologies in the Writing Process

During the preparation of this work the authors used chatgbt in order to improve the readability and language of the manuscript. After using this tool/service, the authors reviewed and edited the content as needed and take full responsibility for the content of the publication.

References:

[1] H. Heidarzadeh, A. Rostami, and M. Dolatyari, "Management of losses (thermalization-transmission) in the Si-QDs inside 3C–SiC to design an ultra-high-efficiency solar cell," *Materials Science in Semiconductor Processing*, vol. 109, p. 104936, Jan. 2020, doi: 10.1016/j.mssp.2020.104936.

[2] H. M. Ali, "Recent advancements in PV cooling and efficiency enhancement integrating phase change materials based systems – A comprehensive review," *Solar Energy*, vol. 197, pp. 163–198, Jan. 2020, doi: 10.1016/j.solener.2019.11.075.

[3] S. Shittu, G. Li, X. Tang, X. Zhao, X. Ma, and A. Badiei, "Analysis of thermoelectric geometry in a concentrated photovoltaic-thermoelectric under varying weather conditions," *Energy*, vol. 202, p. 117742, Apr. 2020, doi: 10.1016/j.energy.2020.117742.

[4] S. Ezzitouni, P. Fernández-Yáñez, L. Sánchez, and O. Armas, "Global energy balance in a diesel engine with a thermoelectric generator," *Applied Energy*, vol. 269, p. 115139, May 2020, doi: 10.1016/j.apenergy.2020.115139.

[5] W. G. J. H. M. Van Sark, "Feasibility of photovoltaic – Thermoelectric hybrid modules," *Applied Energy*, vol. 88, no. 8, pp. 2785–2790, Mar. 2011, doi: 10.1016/j.apenergy.2011.02.008.

[6] X.-Z. Guo, Y.-D. Zhang, D. Qin, Y.-H. Luo, D.-M. Li, Y.-T. Pang, Q.-B. Meng, "Hybrid tandem solar cell for concurrently converting light and heat energy with utilization of full solar spectrum," *Journal of Power Sources*, vol. 195, no. 22, pp. 7684–7690, May 2010, doi: 10.1016/j.jpowsour.2010.05.033.

[7] N. Wang, L. Han, H. He, N.-H. Park, and K. Koumoto, "A novel high-performance photovoltaic–thermoelectric hybrid device," *Energy & Environmental Science*, vol. 4, no. 9, p. 3676, Jan. 2011, doi: 10.1039/c1ee01646f.

[8] D. Yang and H. Yin, "Energy conversion efficiency of a novel hybrid solar system for photovoltaic, thermoelectric, and heat utilization," *IEEE Transactions on Energy Conversion*, vol. 26, no. 2, pp. 662–670, Mar. 2011, doi: 10.1109/tec.2011.2112363.

[9] A.Makki, S. Omer, Y. Su, and H. Sabir, "Numerical investigation of heat pipe-based photovoltaic–thermoelectric generator (HP-PV/TEG) hybrid system," *Energy Conversion and Management*, vol. 112, pp. 274–287, Jan. 2016, doi: 10.1016/j.enconman.2015.12.069.

[10] J. Lin, T. Liao, and B. Lin, "Performance analysis and load matching of a photovoltaic–thermoelectric hybrid system," *Energy Conversion and Management*, vol. 105, pp. 891–899, Sep. 2015, doi: 10.1016/j.enconman.2015.08.054.

[11] D. Kraemer, L. Hu, A. Muto, X. Chen, G. Chen, and M. Chiesa, "Photovoltaic-thermoelectric hybrid systems: A general optimization methodology," *Applied Physics*

Letters, vol. 92, no. 24, Jun. 2008, doi: 10.1063/1.2947591.

[12] M. Mizoshiri, M. Mikami, and K. Ozaki, "Thermal–Photovoltaic hybrid solar generator using Thin-Film thermoelectric modules," *Japanese Journal of Applied Physics*, vol. 51, no. 6S, p. 06FL07, Jun. 2012, doi: 10.7567/jjap.51.06fl07.

[13] X. Ju, Z. Wang, G. Flamant, P. Li, and W. Zhao, "Numerical analysis and optimization of a spectrum splitting concentration photovoltaic–thermoelectric hybrid system," *Solar Energy*, vol. 86, no. 6, pp. 1941–1954, Apr. 2012, doi: 10.1016/j.solener.2012.02.024.

[14] Y. Li, S. Witharana, H. Cao, M. Lasfargues, Y. Huang, and Y. Ding, "Wide spectrum solar energy harvesting through an integrated photovoltaic and thermoelectric system," *Particuology*, vol. 15, pp. 39–44, Nov. 2013, doi: 10.1016/j.partic.2013.08.003.

[15] E. Elsarrag, H. Pernau, J. Heuer, N. Roshan, Y. Alhorr, and K. Bartholomé, "Spectrum splitting for efficient utilization of solar radiation: a novel photovoltaic–thermoelectric power generation system," *Renewables Wind Water and Solar*, vol. 2, no. 1, Nov. 2015, doi: 10.1186/s40807-015-0016-y.

[16] E. J. H. Skjølstrup and T. Søndergaard, "Design and optimization of spectral beamsplitter for hybrid thermoelectric-photovoltaic concentrated solar energy devices," *Solar Energy*, vol. 139, pp. 149–156, Oct. 2016, doi: 10.1016/j.solener.2016.09.036.

[17] E. Yin, Q. Li, and Y. Xuan, "A novel optimal design method for concentration spectrum splitting photovoltaic–thermoelectric hybrid system," *Energy*, vol. 163, pp. 519–532, Aug. 2018, doi: 10.1016/j.energy.2018.08.138.

[18] T. Liao, B. Lin, and Z. Yang, "Performance characteristics of a low concentrated photovoltaic–thermoelectric hybrid power generation device," *International Journal of Thermal Sciences*, vol. 77, pp. 158–164, Dec. 2013, doi: 10.1016/j.ijthermalsci.2013.10.013.

[19] T.-H. Kil, S. Kim, D.-H. Jeong, D.-M. Geum, S. Lee, S.-J. Jung, S. Kim, C. Park, J.-S. Kim, J.M. Baik, K.-S. Lee, C.Z. Kim, W.J. Choi, S.-H. Baek, "A highly-efficient, concentrating-photovoltaic/thermoelectric hybrid generator," *Nano Energy*, vol. 37, pp. 242–247, May 2017, doi: 10.1016/j.nanoen.2017.05.023.

[20] Y.-Y. Wu, S.-Y. Wu, and L. Xiao, "Performance analysis of photovoltaic–thermoelectric hybrid system with and without glass cover," *Energy Conversion and Management*, vol. 93, pp. 151–159, Jan. 2015, doi: 10.1016/j.enconman.2015.01.013.

[21] A.Rezania and L. A. Rosendahl, "Feasibility and parametric evaluation of hybrid concentrated photovoltaic-thermoelectric system," *Applied Energy*, vol. 187, pp. 380–389, Nov. 2016, doi: 10.1016/j.apenergy.2016.11.064.

[22] T. Cui, Y. Xuan, and Q. Li, "Design of a novel concentrating photovoltaic–thermoelectric system incorporated with phase change materials," *Energy Conversion and Management*, vol. 112, pp. 49–60, Jan. 2016, doi: 10.1016/j.enconman.2016.01.008.

[23] T. Cui, Y. Xuan, E. Yin, Q. Li, and D. Li, "Experimental investigation on potential of a concentrated photovoltaic-thermoelectric system with phase change materials," *Energy*, vol. 122, pp. 94–102, Jan. 2017, doi: 10.1016/j.energy.2017.01.087.

[24] M. Mohamed, S. H. Mounir, K. Choukairy, and K. Khallaki, "Performance estimation of the hybridization of crystalline silicon cell with thermoelectric generator," *AIP Conference Proceedings*, vol. 2056, p. 020018, Jan. 2018, doi: 10.1063/1.5084991.

[25] A.Rezania, D. Sera, and L. A. Rosendahl, "Coupled thermal model of photovoltaic-thermoelectric hybrid panel for sample cities in Europe," *Renewable Energy*, vol. 99, pp. 127–135, Jun. 2016, doi: 10.1016/j.renene.2016.06.045.

[26] M. Hammami, S. Torretti, F. Grimaccia, and G. Grandi, "Thermal and Performance Analysis of a Photovoltaic Module with an Integrated Energy Storage System," *Applied Sciences*, vol. 7, no. 11, p. 1107, Oct. 2017, doi: 10.3390/app7111107.

[27] C. Schwingshackl, M. Petitta, J.E. Wagner, G. Belluardo, D. Moser, M. Castelli, M. Zebisch, A. Tetzlaff, "Wind effect on PV module temperature: Analysis of different techniques for an accurate estimation," *Energy Procedia*, vol. 40, pp. 77–86, Jan. 2013, doi: 10.1016/j.egypro.2013.08.010.

[28] J. A. Palyvos, "A survey of wind convection coefficient correlations for building envelope energy systems' modeling," *Applied Thermal Engineering*, vol. 28, no. 8–9, pp. 801–808, Jan. 2008, doi: 10.1016/j.applthermaleng.2007.12.005.

[29] A. Bejan and A. D. Kraus, *Heat transfer handbook*. John Wiley & Sons, 2003.

[30] R. Lamba and S. C. Kaushik, "Modeling and performance analysis of a concentrated photovoltaic–thermoelectric hybrid power generation system," *Energy Conversion and Management*, vol. 115, pp. 288–298, Mar. 2016, doi: 10.1016/j.enconman.2016.02.061.

[31] G. Notton, C. Cristofari, M. Mattei, and P. Poggi, "Modelling of a double-glass photovoltaic module using finite differences," *Applied Thermal Engineering*, vol. 25, no. 17–18, pp. 2854–2877, Apr. 2005, doi: 10.1016/j.applthermaleng.2005.02.008.

[32] A.I. Kudish, E. G. Evseev, G. Walter, and T. Leukefeld, "Simulation study of a solar collector with a selectively coated polymeric double walled absorber plate," *Energy Conversion and Management*, vol. 43, no. 5, pp. 651–671, Mar. 2002, doi: 10.1016/s0196-8904(01)00066-8.

[33] H. Nowak, "The sky temperature in net radiant heat loss calculations from low-sloped roofs," *Infrared Physics*, vol. 29, no. 2–4, pp. 231–232, May 1989, doi: 10.1016/0020-0891(89)90055-9.

[34] S. Manikandan and S. C. Kaushik, "The influence of Thomson effect in the performance optimization of a two stage thermoelectric generator," *Energy*, vol. 100, pp. 227–237, Feb. 2016, doi: 10.1016/j.energy.2016.01.092.

[35] M. Mejdal, M. Nfaoui, Y. Werzgan, A. E. Harfouf, A. Bougtaib, and S. Hayani-Mounir, "Enhancing Efficiency of Photovoltaic-Thermoelectric Hybrid System through Optical Concentrator," *2024 4th International Conference on Innovative Research in Applied Science, Engineering and Technology (IRASET), FEZ*, Morocco, pp. 1–6, May 2024, doi: 10.1109/iraset60544.2024.10549228.

Contribution of Individual Authors to the Creation of a Scientific Article (Ghostwriting Policy)

- M. Mejdal: Conceptualization, Formal analysis, Investigation, Methodology, Project administration, Resources, Validation, Writing – original draft, Data curation, Software, Visualization.
- A. El harfouf: Conceptualization, Formal analysis, Investigation, Methodology, Project administration, Resources, Validation, Writing – review & editing.
- M. Nfaoui: Conceptualization, Investigation, Project administration, Writing – review & editing.
- S. Hayani Mounir and K. Choukairy: Conceptualization, Formal analysis, Investigation, Methodology, Project administration, Resources, Validation, Writing – review & editing.
- K. El hami: Conceptualization, Investigation, Project administration, Supervision, Writing – review & editing.

Sources of Funding for Research Presented in a Scientific Article or Scientific Article Itself
No funding was received for conducting this study.

Conflict of Interest
The authors have no conflicts of interest to declare.

APPENDIX

Table 3. Distribution of the dominance of each type of energy loss in the PV-TEG hybrid system depending on meteorological factors

		low radiation high Wind high temperature	high radiation low Wind low temperature	high Wind high radiation high temperature	low Wind low radiation low temperature	low Wind high radiation high temperature	low radiation high Wind low temperature
PV-TEG without concentration	Forced convection	Dominant	Dominant	Dominant	--------	--------	Dominant
	Radiation	--------	--------	Dominant	Dominant	Dominant	--------
PV-TEG with concentration	Forced convection	--------	--------	--------	--------	--------	--------
	Radiation	Dominant	Dominant	Dominant	Dominant	Dominant	Dominant